Supplementary Information

Investigating Dry Room Compatibility of Sulfide Solid-State Electrolytes for Scalable Manufacturing

Yu-Ting Chen[1], Maxwell A. T. Marple[2], Darren H. S. Tan[3], So-Yeon Ham[1], Baharak Sayahpour[1], Wei-Kang Li[3], Hedi Yang[3], Jeong Beom Lee[4], Hoe Jin Hah[4], Erik A. Wu[3], Jean-Marie Doux[3], Jihyun Jang[3], Phillip Ridley[3], Ashley Cronk[1], Grayson Deysher[1], Zheng Chen[1,3,5,6]*, and Ying Shirley Meng[1,3,5]*

[1] Program of Materials Science and Engineering, University of California San Diego, La Jolla, California 92093, United States

[2] Physical and Life Science Directorate, Lawrence Livermore National Laboratory, Livermore, California 94550, United States

[3] Department of NanoEngineering, University of California San Diego, La Jolla, California 92093, United States of America

[4] LG Energy Solution, Ltd., LG Science Park, Magokjungang 10-ro, Gangseo-gu, Seoul 07796, Korea.

[5] Sustainable Power & Energy Center (SPEC), University of California San Diego, La Jolla, California 92093, United States

[6] Program of Chemical Engineering, University of California San Diego, La Jolla, California 92093, United States

* shmeng@ucsd.edu (Y. S. M.), zhengchen@eng.ucsd.edu (Z. C.)

This PDF file includes

Figure S1 to S19

Table S1 to S6

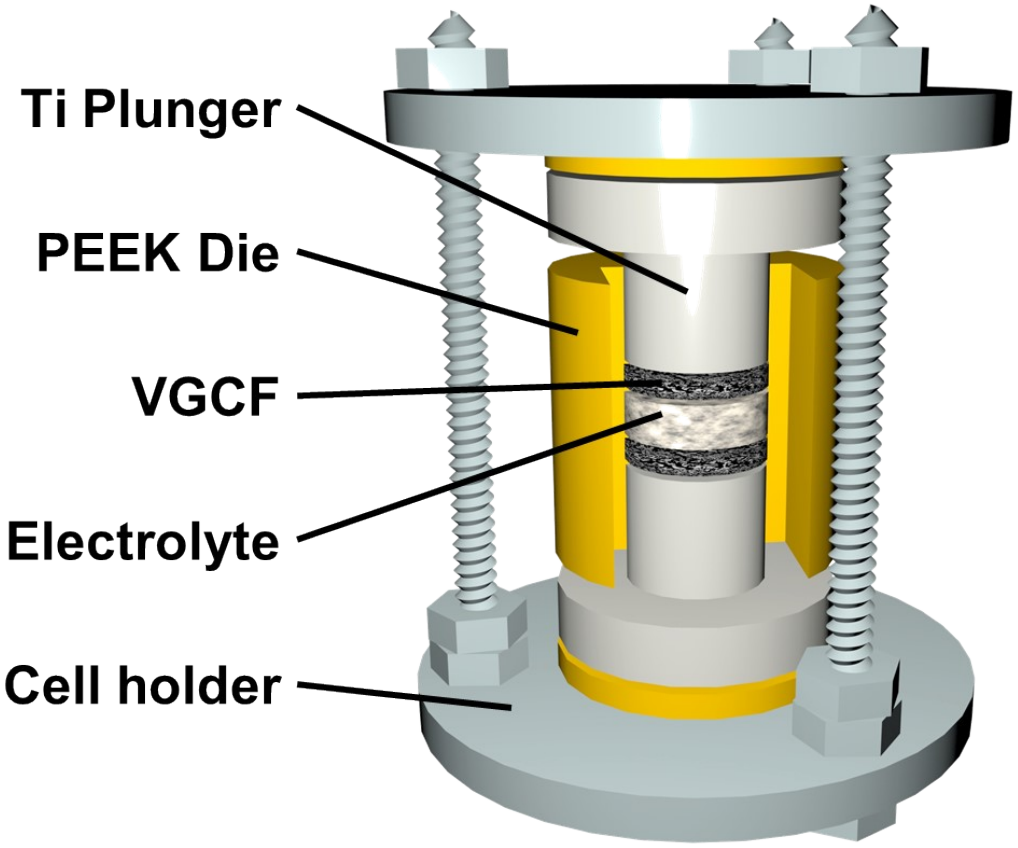

Figure S1. The design of an EIS cell used in this work.

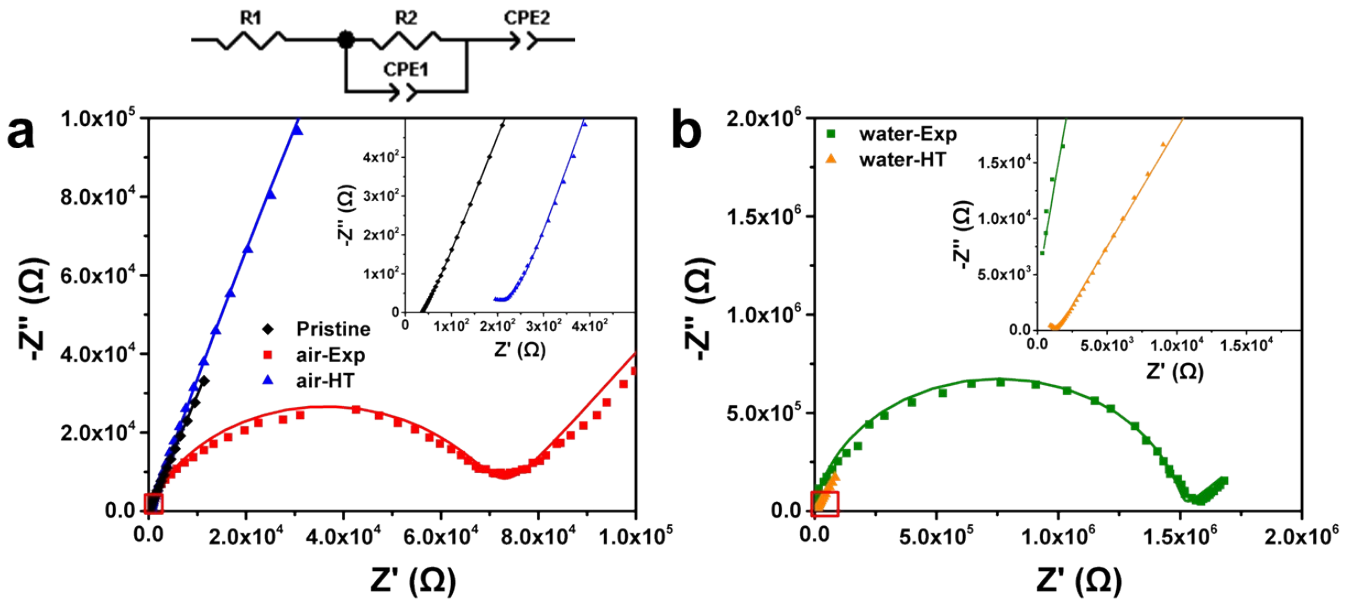

Figure S2. The Nyquist plots of a) pristine, air-Exp, air-HT, b) water-Exp and water-HT LPSCl samples.

Table S1. The EIS fitting results of pristine, air-EXP, air-HT, water-Exp and water-HT LPSCl samples.

Sample	$R_1 + R_2$	CPE_1-T	CPE_1-P	CPE_2-T	CPE_2-P
Pristine	2.86×10^{1}			6.85×10^{-8}	9.16×10^{-1}
air-Exp	7.10×10^{4}	1.46×10^{-9}	8.05×10^{-1}	1.59×10^{-6}	6.01×10^{-1}
air-HT	2.79×10^{2}	1.83×10^{-6}	1.98×10^{-1}	4.73×10^{-7}	8.25×10^{-1}
water-Exp	1.50×10^{6}	6.74×10^{-11}	9.29×10^{-1}	1.66×10^{-6}	5.04×10^{-1}
water-HT	1.45×10^{3}	5.45×10^{-10}	4.19×10^{-1}	1.43×10^{-6}	7.18×10^{-1}

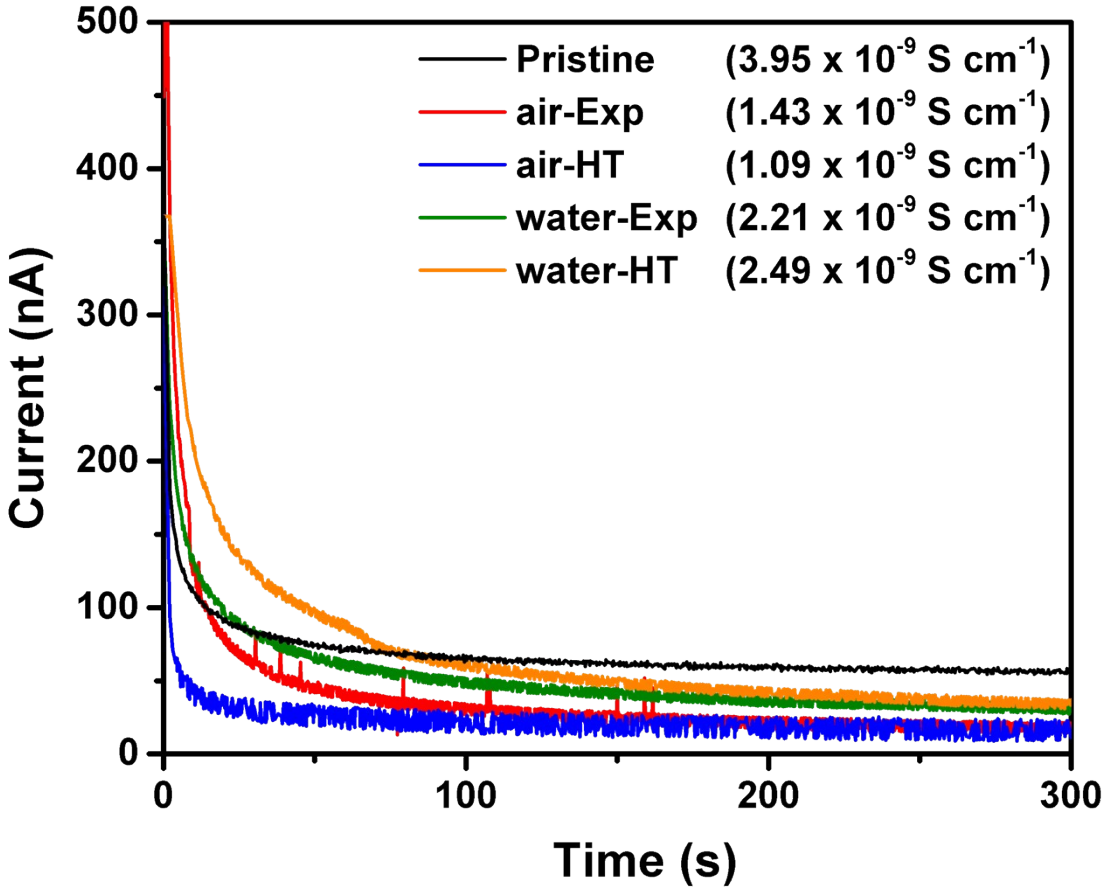

Figure S3. The DC polarization plots (applying 1 V bias) of the pristine, air, and water exposed LPSCl samples before and after heat treatment. Their electronic conductivities are of 10^{-9} S cm^{-1} order.

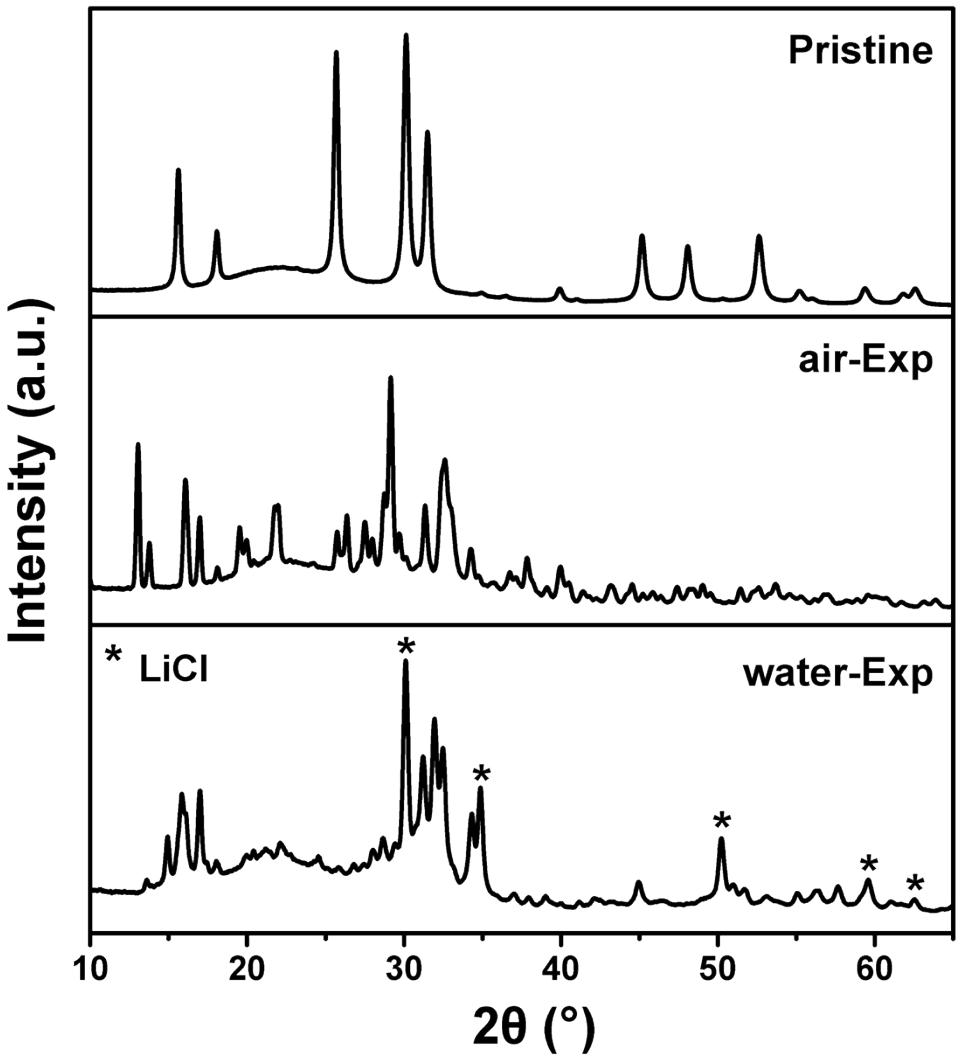

Figure S4. The XRD patterns of pristine, air and water exposed LPSCl samples.

Table S2. The Rietveld refinement results of phase ratios and unit cells of air-HT and water-HT.

air-HT		Unit Cell					
Phase	Phase ratio (%)	a (Å)	b (Å)	c (Å)	α (°)	β (°)	γ (°)
Li_6PS_5Cl	35.8(3)	9.8550(7)	9.8550(7)	9.8550(7)	90	90	90
Li_2S	22.0(4)	5.713(1)	5.713(1)	5.713(1)	90	90	90
LiCl	22.0(4)	5.1522(7)	5.1522(7)	5.1522(7)	90	90	90
Li_3PO_4	20.4(3)	6.119(2)	10.487(3)	4.3926(1)	90	90	90

water-HT		Unit Cell					
Phase	Phase ratio (%)	a (Å)	b (Å)	c (Å)	α (°)	β (°)	γ (°)
Li_6PS_5Cl	8.2(8)	9.8924(7)	9.8924(7)	9.8924(7)	90	90	90
Li_2S	31.4(2)	5.7252(4)	5.7252(4)	5.7252(4)	90	90	90
LiCl	28.3(2)	5.1690(3)	5.1690(3)	5.1690(3)	90	90	90
Li_3PO_4	32.1(2)	6.1374(6)	10.513(1)	4.9358(4)	90	90	90

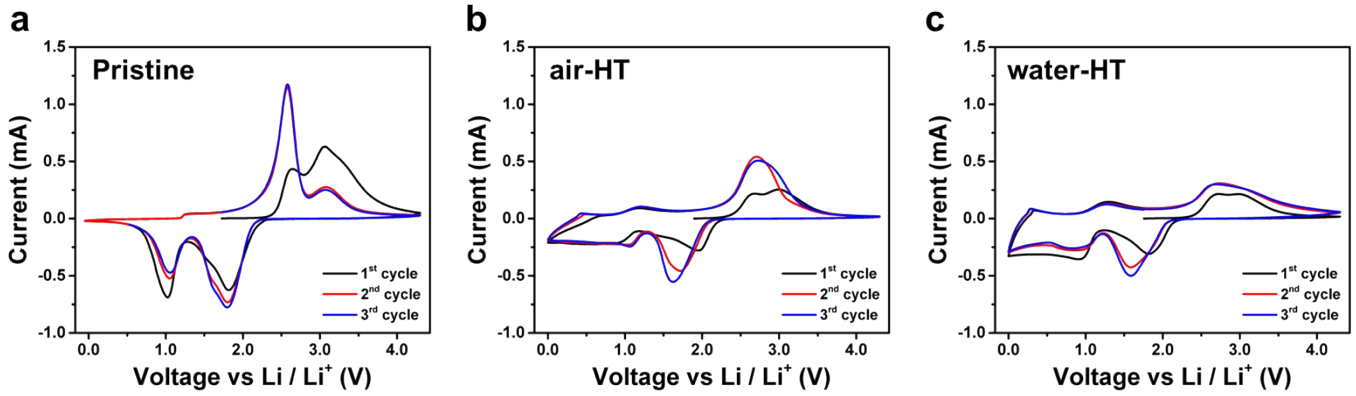

Figure S5. The cyclic voltammetry of a) pristine, b) air-HT, and c) water-HT LPSCl samples.

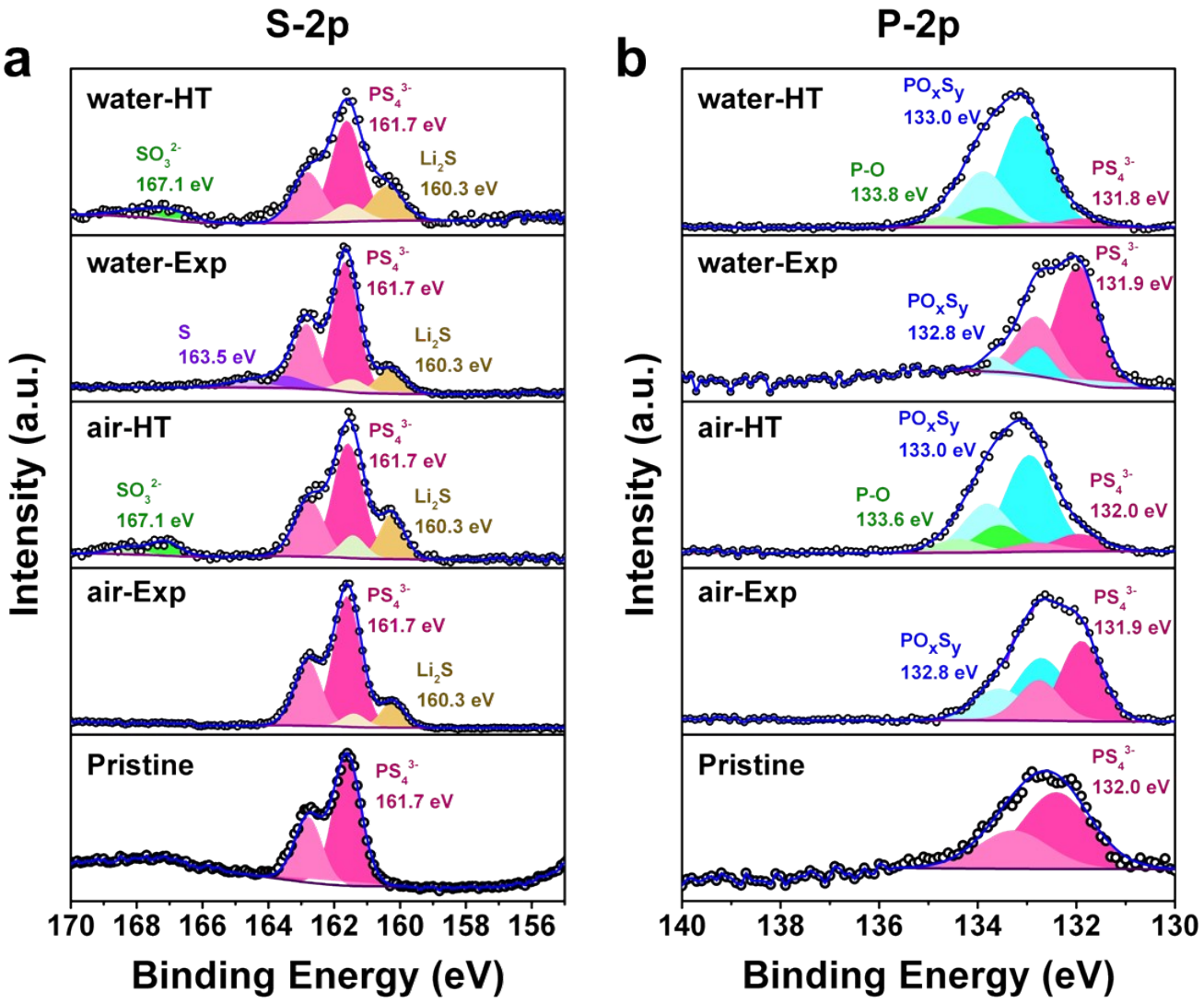

Figure S6. The a) S 2*p* and b) P 2*p* XPS of the pristine, air, and water exposed LPSCl samples before and after heat treatment.

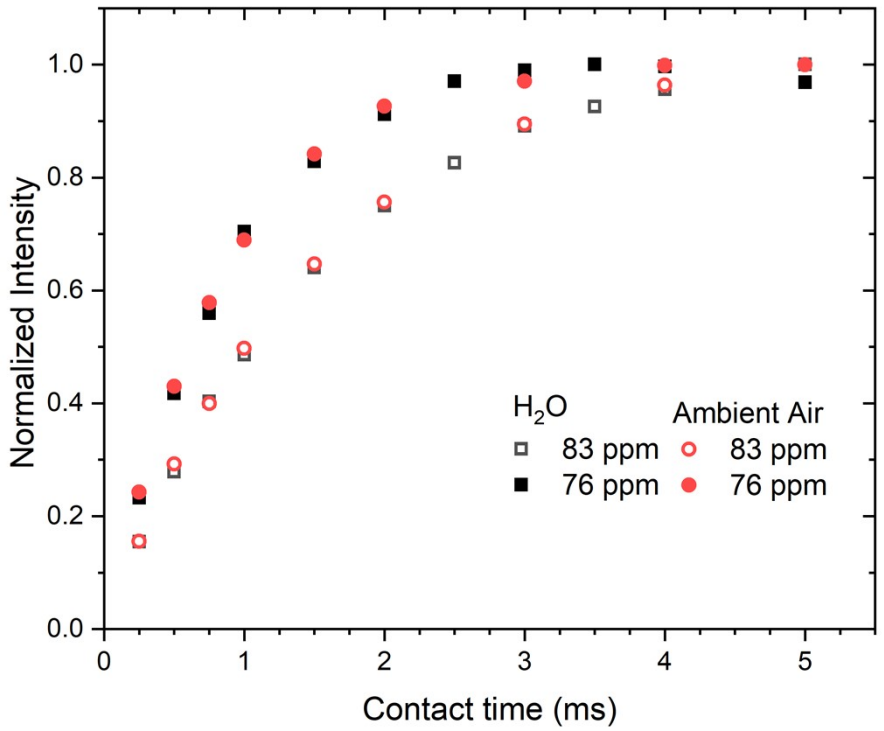

Figure S7. {^{1}H}-^{31}P cross polarization build-up curves from variable contact time measurements. The signal is normalized to highest intensity of each peak. The 83 and 76 ppm peaks have identical CP kinetics across the two samples indicating they are the same phases.

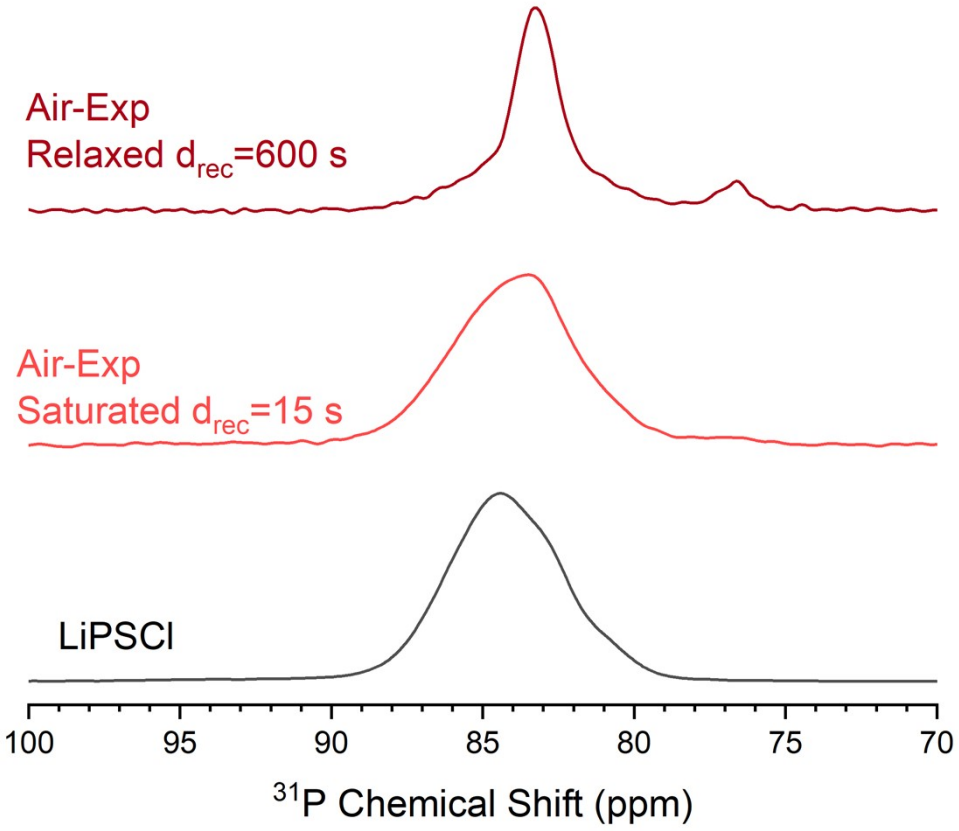

Figure S8. ^{31}P spectra of pristine LPSCl (bottom) and air exposed LPSCl collected with a short recycle delay (middle), and long recycle delay (top). Using a short recycle delay saturates the signal of the slowly relaxing phases and makes the signal of the LPSCl clearly observable.

Table S3. NMR fitting results for pristine and exposed LPSCl.

^{31}P Site	δ_{iso} (ppm)	δ_{width} (ppm)	%	Total Recovered Li_6PS_5Cl (%)	^{31}P SLR T_1 (s)	^{7}Li SLR T_1 (s)
Pristine Li_6PS_5Cl						
Li_6PS_5Cl PS_4^{3-}	85.01	3.66	59			
Li_6PS_5Cl PS_4^{3-}	83.13	3.53	35		4.0	0.16
Li_6PS_5Cl PS_4^{3-}	80.39	1.85	2			
Li_3PS_4	89.08	12	4		-	
Dry Room Li_6PS_5Cl						
Li_6PS_5Cl PS_4^{3-}	85.03	3.88	60			
Li_6PS_5Cl PS_4^{3-}	83.12	3.55	33		3.4	0.19
Li_6PS_5Cl PS_4^{3-}	80.43	1.85	2			
Li_3PS_4	87.94	11.96	5		-	
Ambient Air						
LPSCl PS_4^{3-}	83.42	5.02	57		3.8	0.18
Hydrated POS_3^{3-}	83.27	1.34	36		386	9
Hydrated $PO_2S_2^{3-}$	76.71	1.32	7		534	(LiCl) 11.7
Ambient Air 550°C						
Li_6PS_5Cl PS_4^{3-}	85.03	3.88	37			
Li_6PS_5Cl PS_4^{3-}	83.12	3.55	28.6	67.4	2.9	0.13
Li_6PS_5Cl PS_4^{3-}	80.43	1.85	1.8			
$PO_2S_2^{3-}$	73.11	3.07	1		-	8.7
PO_3S^{3-}	35.06	2.65	0.6		-	6.9
Li_3PO_4	9.3	1.1	31		765.3	(LiCl) 26.5
H_2O						
Hydrated POS_3^{3-}	83.2	1.48	8		742	(LiCl) 25.5
Hydrated $PO_2S_2^{3-}$	76.78	1.06	92		992	
H_2O 550°C						
Li_6PS_5Cl PS_4^{3-}	85.03	3.88	29			
Li_6PS_5Cl PS_4^{3-}	83.12	3.55	17	47	3.1	0.15
Li_6PS_5Cl PS_4^{3-}	80.46	1.9	1			
$P_2S_7^{4-}$	91.47	2.45	13		346.6	
$PO_2S_2^{3-}$	70.67	9.17	4		324.5	
PO_3S^{3-}	35.74	6.53	8		433.4	
PO_4^{3-}	11.03	1.96	6		398.6	
Li_3PO_4	9.47	1.68	22		447.7	(LiCl) 25.7

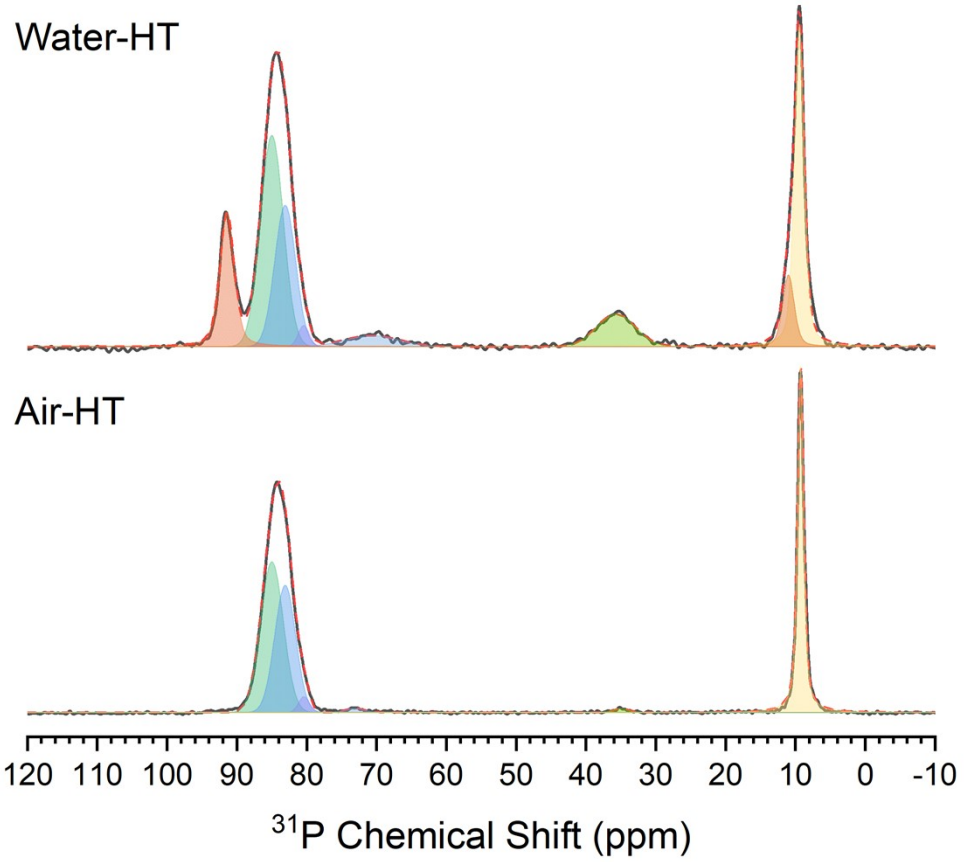

Figure S9. Closer view of the ^{31}P spectra of the heat-treated samples to more clearly show the minor oxysulfide phases still present.

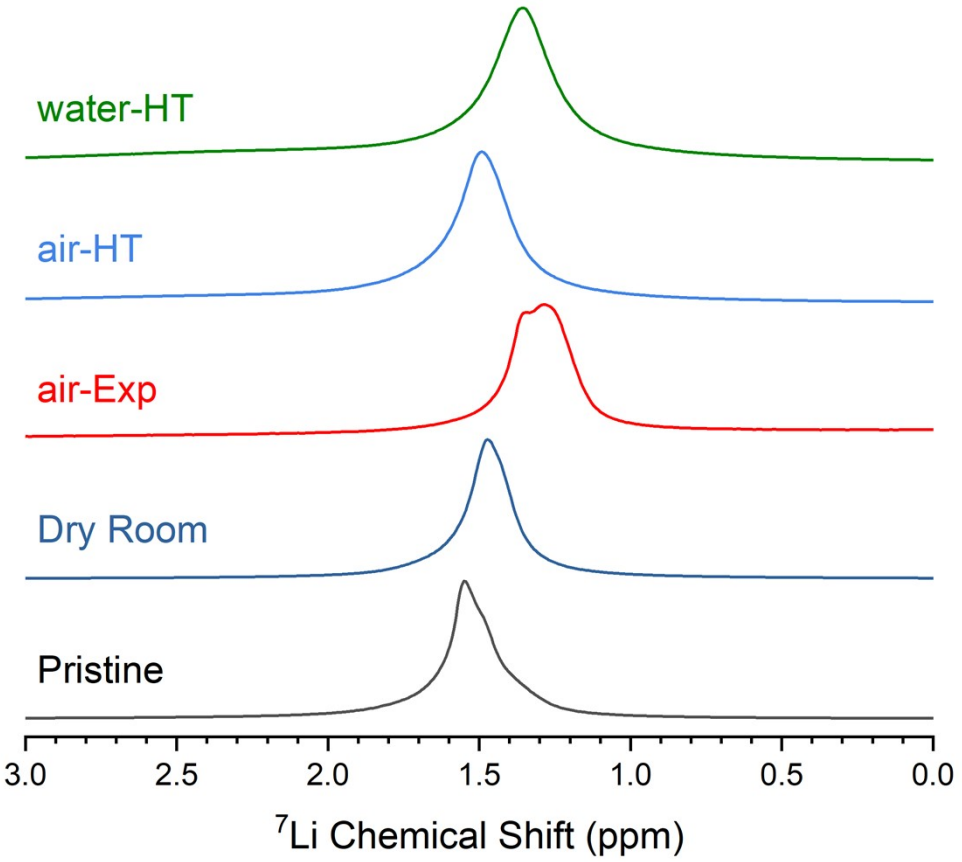

Figure S10. ^{7}Li spectra focused on the chemical shift range around LPSCl. The water exposed sample is omitted because it lacks a LPSCl signal and its breadth is beyond the axis scale.

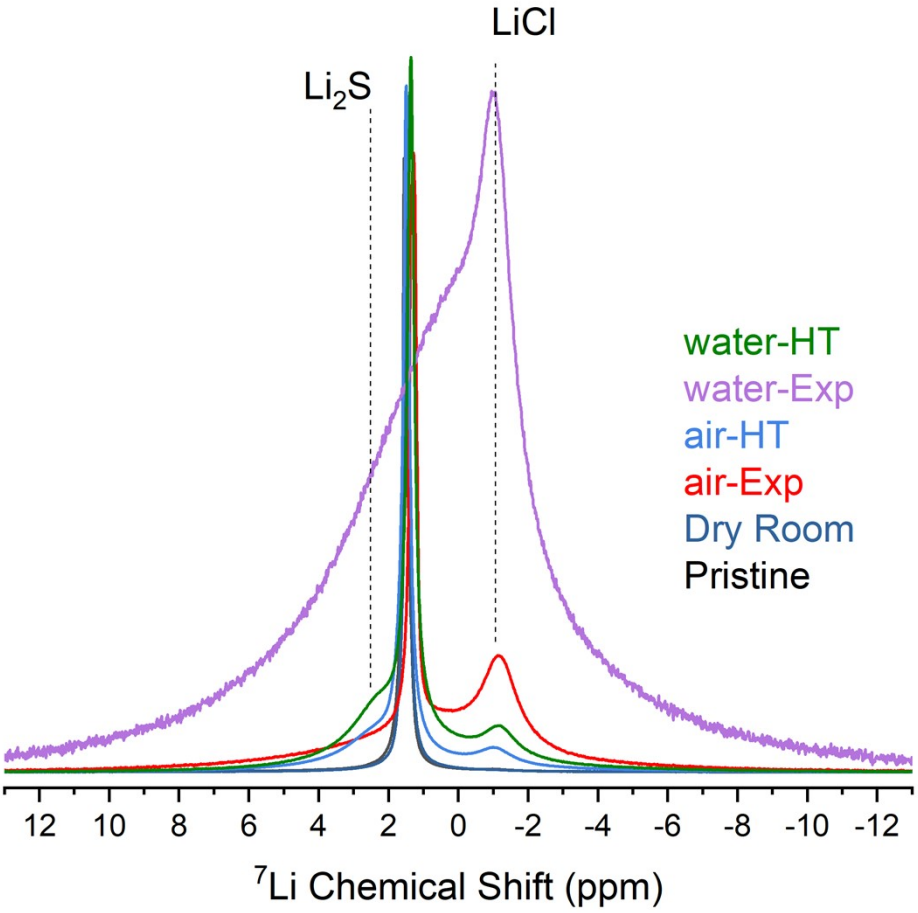

Figure S11. An overlay plot of all ^{7}Li spectra to show the progressive increase of LiCl and Li_2S after exposure and heat-treatment.

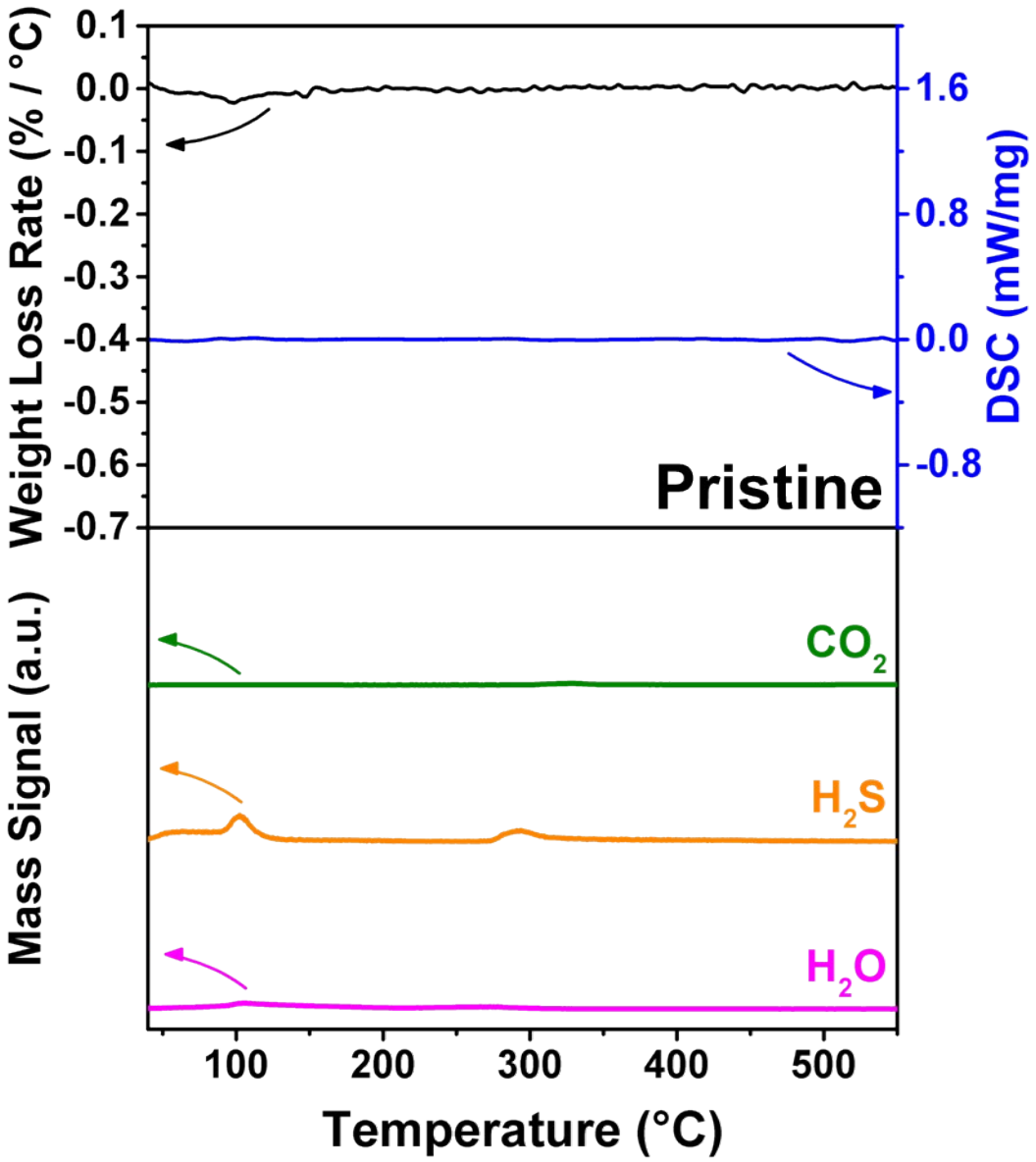

Figure S12. The TGA / DSC – MS of pristine LPSCl. No obvious mass loss and DSC signal were observed. Due to short exposure to air during the sample preparation, there are slight H_2S and H_2O evolution.

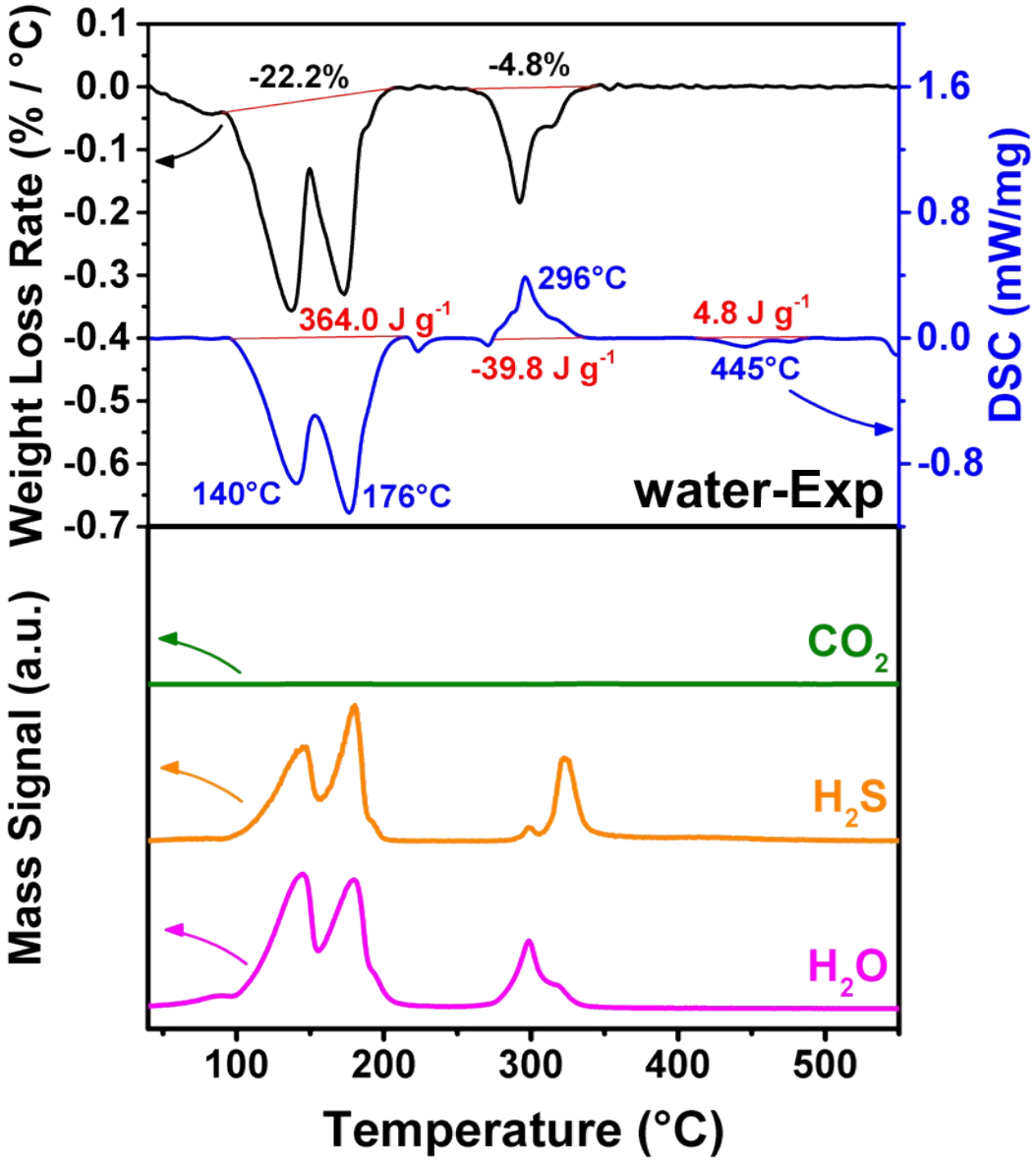

Figure S13. The TGA / DSC – MS of water-exposed LPSCl (water-Exp).

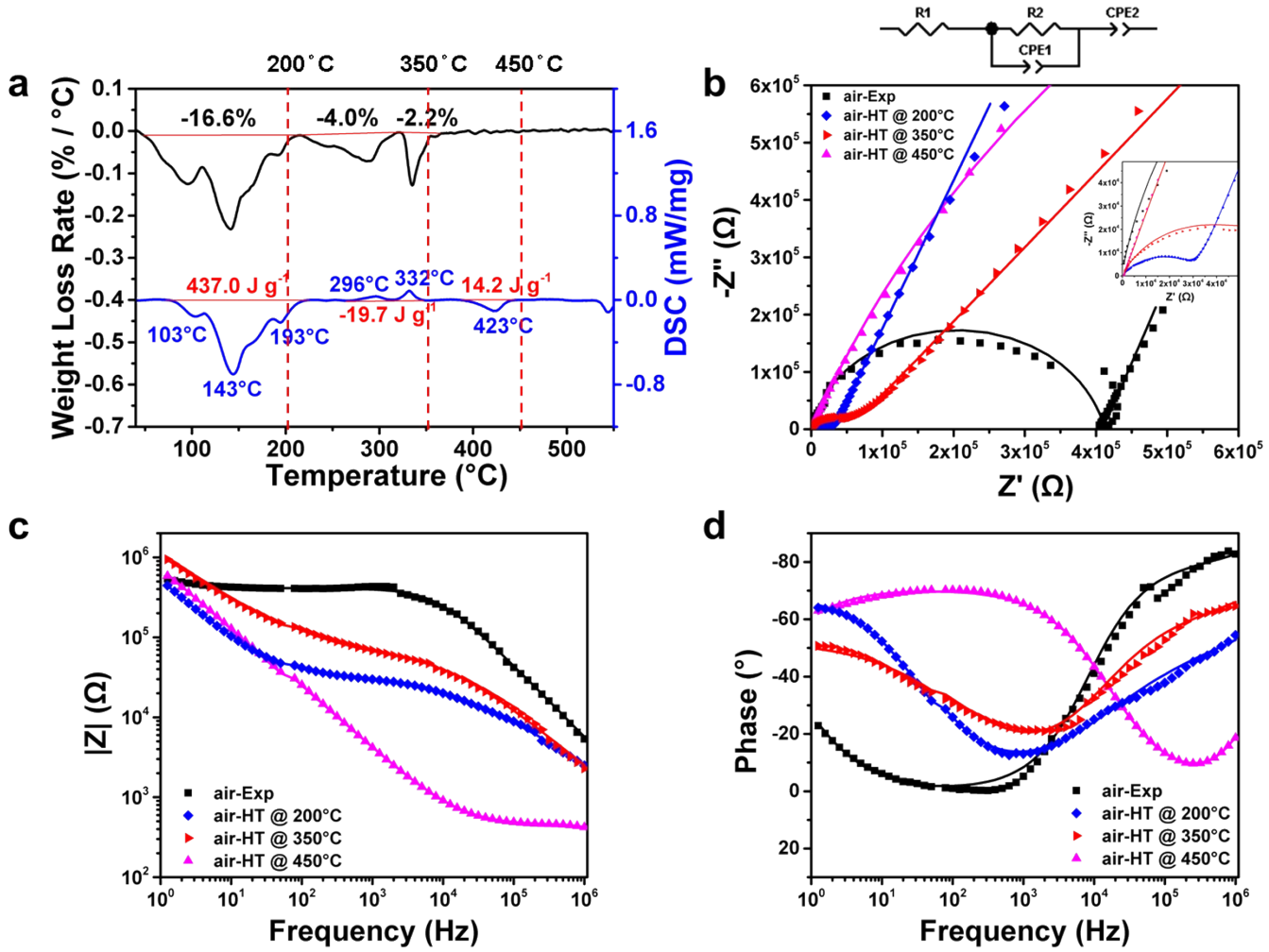

Figure S14. According to a) TGA / DSC – Mass result, AIR was heat treated at lower temperatures: 200, 350 and 450°C for 8 hours and the b) Cole-Cole plot, c) magnitude and d) phase of Bode plots of air-Exp sample heat treated at all temperature were measured.

Table S4. The EIS fitting results of air-EXP and air-HT samples heat treated at 200, 350 and 450°C.

Sample	$R_1 + R_2$	CPE_1-T	CPE_1-P	CPE_2-T	CPE_2-P
air-Exp	7.10×10^{4}	1.46×10^{-9}	8.05×10^{-1}	1.59×10^{-6}	6.01×10^{-1}
air-HT @ 200°C	3.23×10^{4}	4.70×10^{-8}	5.68×10^{-1}	4.03×10^{-7}	7.65×10^{-1}
air-HT @ 350°C	5.52×10^{4}	5.76×10^{-9}	7.17×10^{-1}	2.95×10^{-7}	5.82×10^{-1}
air-HT @ 450°C	4.39×10^{2}	5.76×10^{-11}	7.28×10^{-1}	2.51×10^{-7}	7.87×10^{-1}

Table S5. A summary of ionic conductivity of air-HT heat-treated at 200, 350 and 450°C.

Ionic Conductivity (S cm^{-1})	
Pristine	2.90×10^{-3}
air-Exp	1.72×10^{-7}
200°C	2.17×10^{-6}
350°C	1.26×10^{-6}
450°C	1.59×10^{-4}

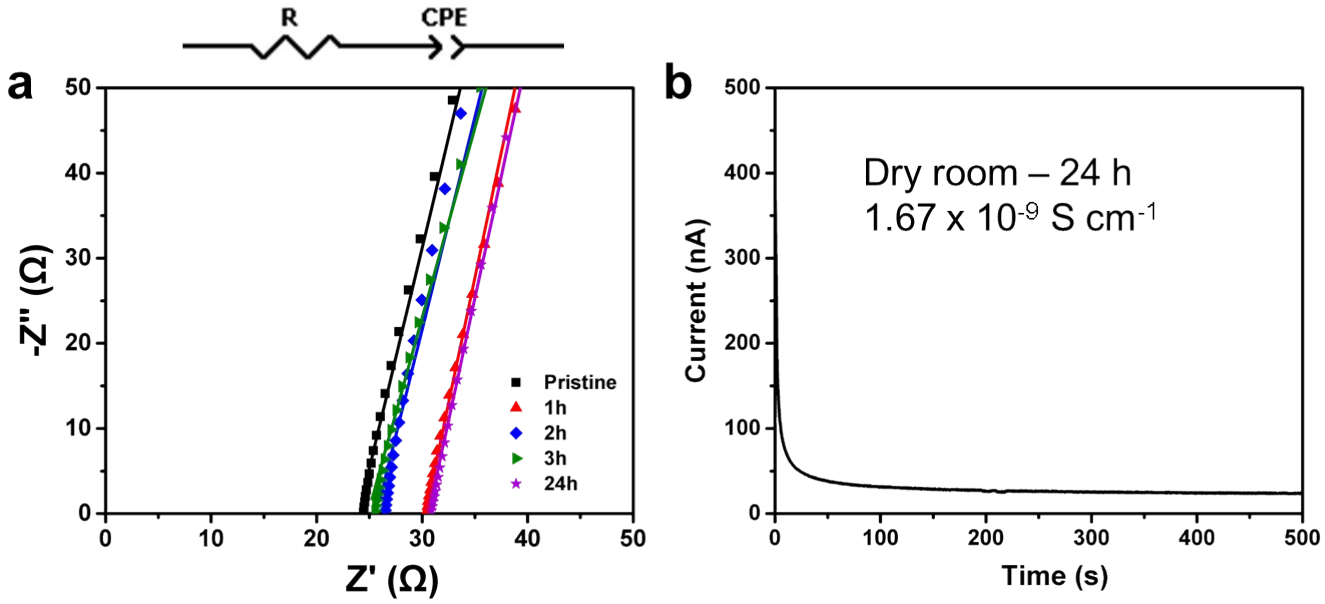

Figure S15. a) The Nyquist plots of LPSCl exposed in a dry room for 1, 2, 3 and 24 hours. b) the DC polarization of LPSCl exposed in a dry room for 24 hours. No significant increase in electronic conductivity was observed.

Table S6. The EIS fitting results of LPSCl samples exposed in a dry room for 1, 2, 3 and 24 hours.

Sample	R	CPE-T	CPE-P
Pristine	2.86×10^{1}	6.85×10^{-8}	9.16×10^{-1}
1 hour	3.03×10^{1}	2.01×10^{-6}	8.93×10^{-1}
2 hours	2.57×10^{1}	2.00×10^{-6}	8.74×10^{-1}
3 hours	2.49×10^{1}	3.20×10^{-6}	8.60×10^{-1}
24 hours	3.06×10^{1}	2.20×10^{-6}	8.90×10^{-1}

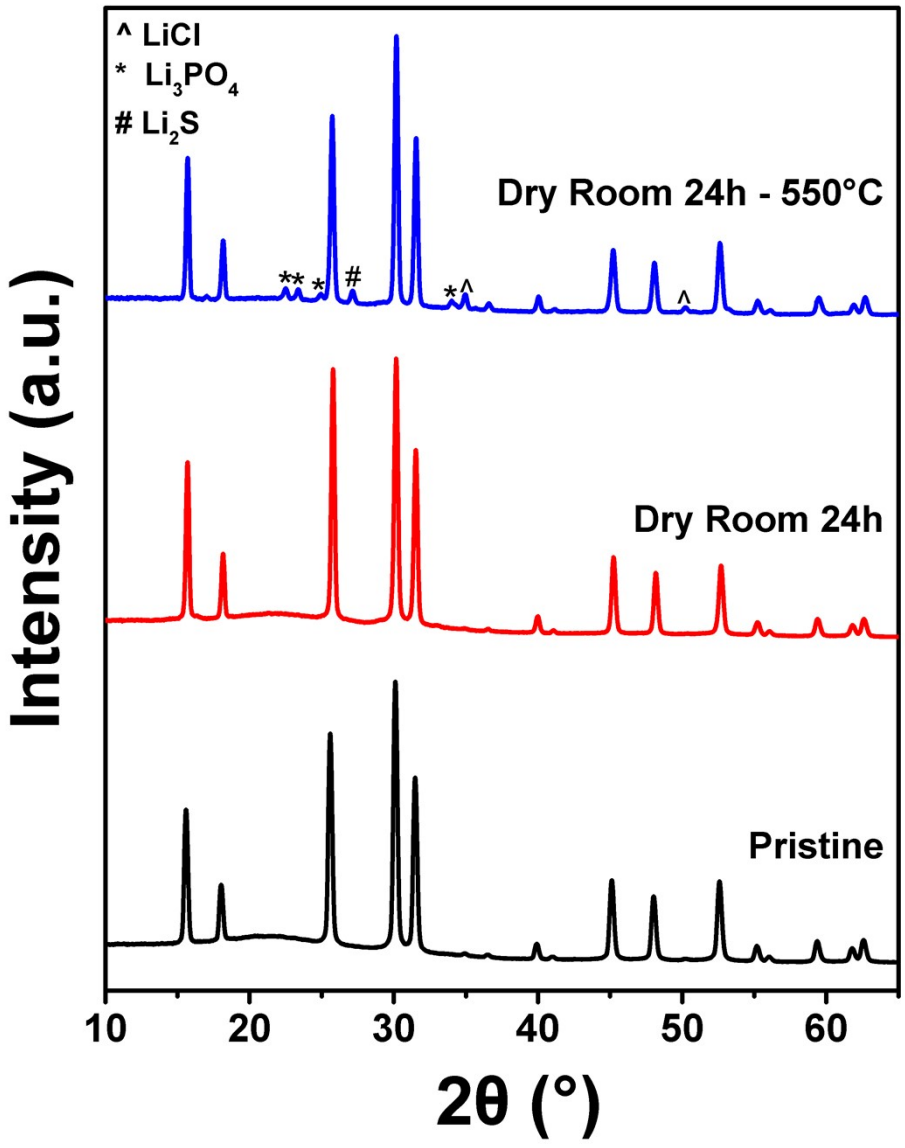

Figure S16. The XRD patterns of pristine LPSCl, LPSCl exposed in a dry room for 24 hours, and followed by a heat treatment at 550°C.

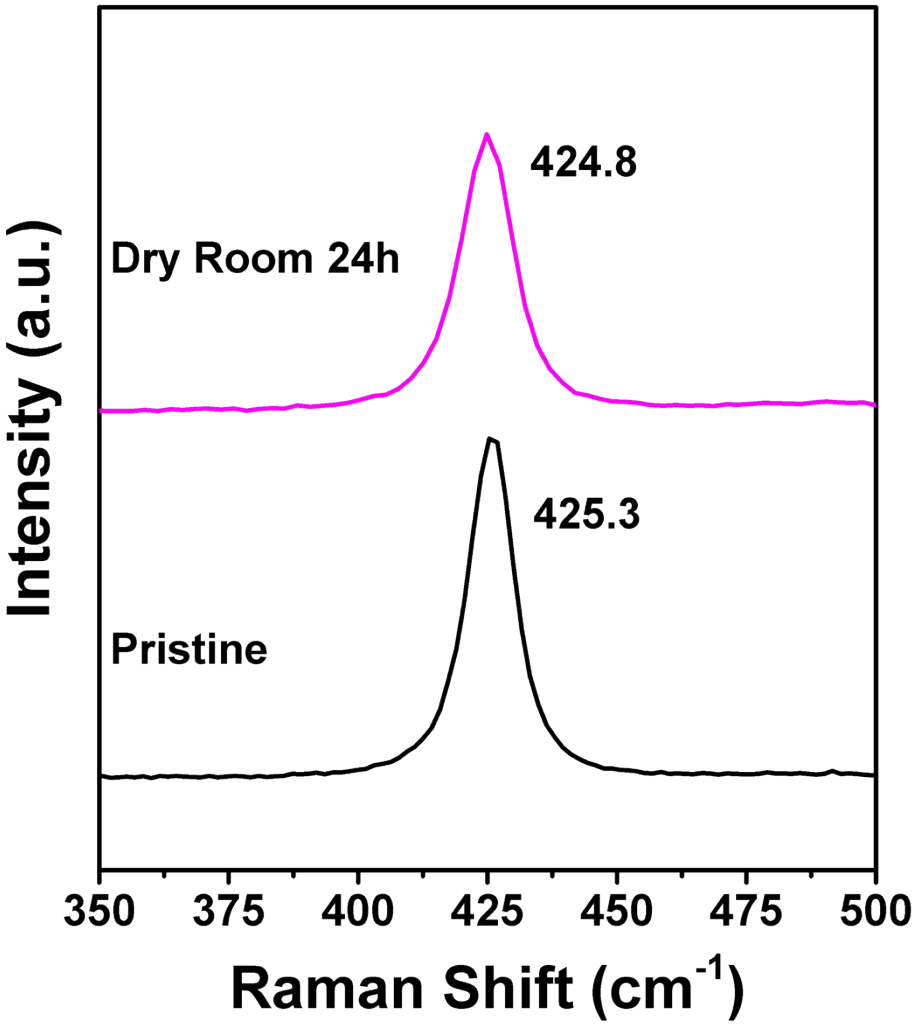

Figure S17. The Raman spectra of pristine LPSCl and after exposing in a dry room for 24 hours.

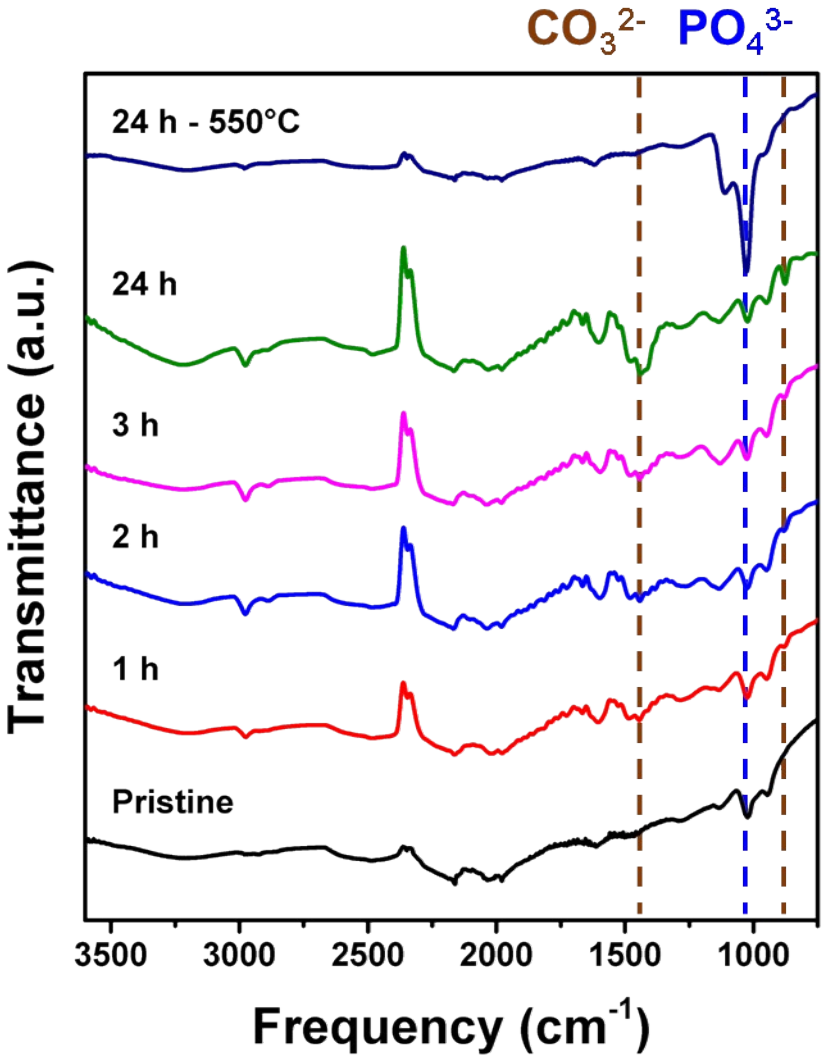

Figure S18. The FTIR spectra of pristine LPSCl and LPSCl exposed in a dry room for 1, 2, 3, 24 hours and followed by a heat treatment at 550°C.

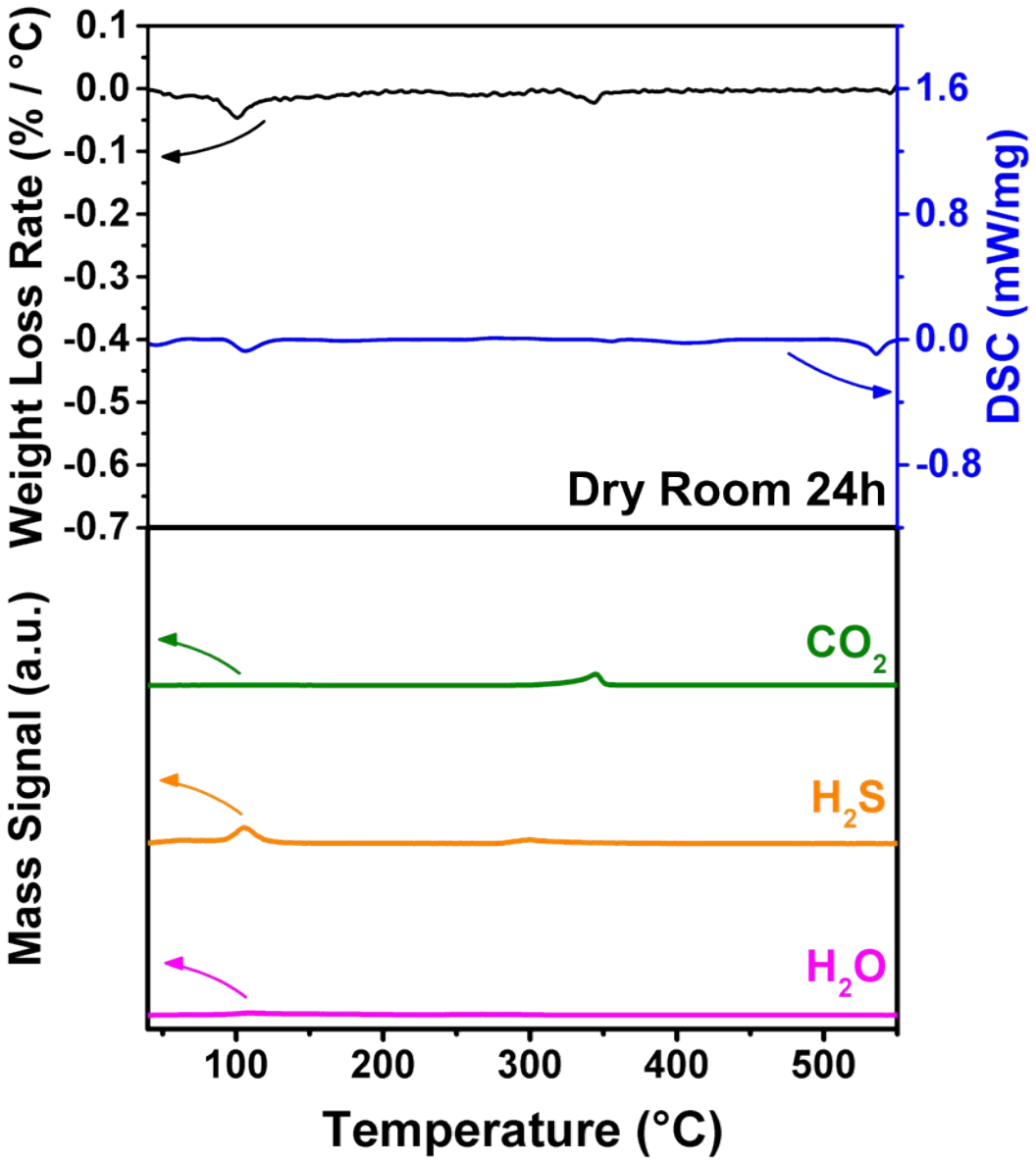

Figure S19. The TGA / DSC – MS of LPSCl exposed in a dry room for 24 hours.